THE JOURNAL OF PHYSICAL CHEMISTRY B

Article

pubs.acs.org/JPCB

Chirality and Packing in Small Proline Clusters

Natalya Atlasevich,[†] Alison E. Holliday,*[,‡] Stephen J. Valentine,[†,§] and David E. Clemmer*[,†]

[†]Department of Chemistry, Indiana University, Bloomington, Indiana 47405, United States

[‡]Department of Chemistry and Biochemistry, Swarthmore College, Swarthmore, Pennsylvania 19081, United States

ABSTRACT: The chiral composition of amino acid clusters may be related to the origin of chirality in biological systems. Here, we use ion mobility/mass spectrometry techniques to investigate the gas phase structures of singly charged proline clusters containing two to six monomers. Using deuterated L-proline (L_{D7}) and different electrospray solution compositions varying from enantiopure (50:50 L:L_{D7}) to racemic (50:50 L_{D7}:D), it is possible to study collision cross sections of L-, D-, and mixed *x*L:*x*D-proline clusters (where *x* refers to the number of monomers). These results show that $[2Pro+H]^+$ and $[3Pro+H]^+$ clusters, previously shown (Holliday et al. *J. Phys. Chem. A* **2012**, DOI: 10.1021/jp302677n) to have a very small heterochiral preference, have similar collision cross sections for homochiral and heterochiral proline assemblies. The $[4Pro+H]^+$ and $[6Pro+H]^+$ clusters that exhibit homochiral preference have smaller collision cross sections for homochiral clusters and larger collision cross sections for heterochiral clusters. The $[5Pro+H]^+$ cluster with heterochiral preference has a smaller collision cross section for its heterochiral compositions than for its homochiral compositions. These results suggest that the packing efficiency of subunits within each cluster influences the stability and prevalence of proline multimers as either homochiral or mixed L- and D-clusters.

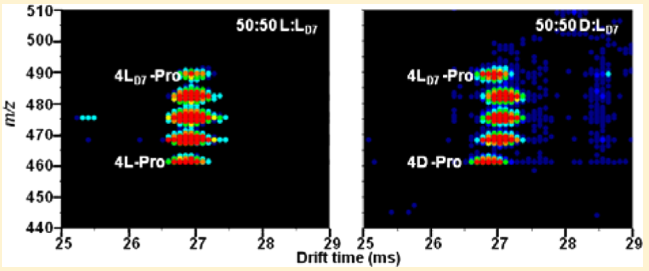

INTRODUCTION

The chiral composition of amino acid clusters is a rich area of study, connected with questions about the origins of chirality in biological systems, and thus the origin of life itself.[1−3] Using mass spectrometry (MS)[4−7] and ion mobility (IMS) MS techniques,[8−14] the favored chiral composition of a number of amino acid clusters has been determined. We have recently begun a study of the chiral preferences of a range of proline clusters,[14,15] discovering an oscillation between strong preference for homochiral structures and that for heterochiral structures as a function of cluster size.[14] For homochirally preferring cluster sizes, the formation of homochiral clusters when spraying racemic solutions exceeds what one would expect from a statistical distribution of cluster chiralities. This occurs despite the fact that homochiral assembly from racemic solutions is entropically[16] disfavored. Thus, homochiral clusters exhibit a special stability for some sizes. Accordingly, potential structures of clusters are proposed based on energy minimization calculations,[4,5,9,17,18] and higher level calculations are now being done for structures of increasingly large clusters.[19] To date, ion mobility has provided the collision cross section data used to give credence to proposed structures, particularly that of the homochiral serine octamer[8,9] and the homochiral proline dodecamer.[13]

When spraying from a racemic solution, a range of different chiral compositions of a given cluster are simultaneously formed. With the use of deuterium-labeled amino acids and high-resolution IMS-MS, it is possible to separately observe each chiral composition of a cluster $[xAA+H]^+$, where *x* is the number of amino acids (AA) in the cluster. This allows the observation of chirally dependent trends in packing of amino acid clusters, as well as the calculation of collisional cross sections for individual species, forming a link between theoretical and experimental structures.

For singly charged clusters of proline, we observe that the most favored structures (based on relative signal intensity) are also the structures that are most compact. Although we do not claim that this trend will hold true for all amino acid clusters, this added dimension of information will prove very useful as more complex systems are explored.

EXPERIMENTAL SECTION

Overview. Ion mobility spectrometry methodology and techniques have been described in detail previously[20−33] and will only be mentioned here briefly. Ions are generated by electrospray ionization (ESI) and are introduced into a differentially pumped source region containing an hourglass ion funnel.[29] Ions are then trapped and gated (150 μs pulse) into the drift tube (~289 cm) filled with ~3.0 Torr of 300 K He buffer gas. The drift tube is operated at the low field limit (~10 V·cm^{-1}) and contains three ion funnels that are used to concentrated diffuse ion clouds. Ions are detected at the back of the drift region with a reflectron geometry time-of-flight mass spectrometer. Because flight times in the mass spectrometer occur on a much shorter time scale than the drift times of ions traversing the drift tube, it is possible to record drift and flight

Received: July 14, 2012
Revised: August 22, 2012
Published: August 23, 2012

times with a nested approach that has been described previously.[26]

Ion drift times can be converted to collision cross sections (Ω) with the expression given in eq 1.[20]

$$\Omega = \frac{(18\pi)^{1/2}}{16}\frac{ze}{(k_bT)^{1/2}}\left[\frac{1}{m_I}+\frac{1}{m_B}\right]^{1/2}\frac{t_DE}{L}\frac{760}{P}\frac{T}{273.2}\frac{1}{N} \quad (1)$$

Here, m_I, and m_B are the masses of the ion and the buffer gas, respectively. The variables ze, E, L, P, and T correspond to an ion's charge, the electric field, the drift tube length, pressure, and the temperature of the buffer gas. N is the neutral number density of the buffer gas at standard temperature and pressure, and k_b is Boltzmann's constant.

Sample Preparation. Solutions with L- and D-proline (Fluka, 99% purity) and deuterated L-proline ($HN(CD_2)_3CD$)-COOH) (Cambridge Isotope Laboratories, Inc., ≥98% purity) were prepared in 49:49:2 water:acetonitrile:acetic acid at a total concentration of 0.01M. Both enantiopure (50:50 L:L_{D7}-proline) and racemic (50:50 L_{D7}:D-proline) solutions were electrosprayed into the instrument with a flow rate of 0.1 μL min^{-1} through a pulled fused silica capillary tip made in house (100 μm i.d., 360 μm o.d., Polymicro). The solution in the capillary tip was biased ca. +2500 V above the ESI desolvation region entrance aperture.

Molecular Modeling. Structures for $[4Pro+H]^+$ and $[5Pro+H]^+$ D-proline clusters were modeled as zwitterions using the InsightII molecular modeling package (Accelrys. Inc. San Diego, CA). The selected D-proline clusters were used as the starting point for building racemic clusters which were constructed by reflecting the desired number of D-proline residues into L-proline. The structures were then energy minimized with the consistent valence forcefield (CVFF) and exported into MOBCAL (developed by Jarrold and co-workers)[34,35] to calculate theoretical collision cross sections using the trajectory method. Average theoretical collision cross sections for $[4Pro+H]^+$ and $[5Pro+H]^+$ clusters were within ±1.5% of the experimental values.

RESULTS

IMS-MS Spectra. Figure 1 shows 10 two-dimensional nested ion mobility distributions for $[xPro+H]^+$ (where x = 2–6) formed from enantiopure (50:50 L:L_{D7}) and racemic (50:50 L_{D7}:D) solutions containing isotopically labeled L-proline (L_{D7}). The incorporation of deuterium allows clusters with the same number of subunits to be separated based on their enantiomeric composition in the m/z dimension. Clusters containing only L- or D-proline have no deuterium incorporated, and are at the lowest m/z values. Clusters containing only L_{D7}-proline have $7x$ deuteriums (where x = number of proline monomers) incorporated and are at the highest m/z values. Between these extremes are found clusters that contain both isotopically labeled and unlabeled proline. Thus, a total of x + 1 distinct peaks (corresponding to 0–x L_{D7} incorporated) can be observed for $[xPro+H]^+$. This approach makes it possible to compare drift times of homochiral clusters and mixed clusters composed of varied L_{D7}- and D-proline ratios.

Proline clusters for $[xPro+H]^+$ (where x = 2 and 3) formed from the enantiopure solution (50:50 L:L_{D7}) have the same drift times for pure L and pure L_{D7} clusters. In contrast, enantiopure proline clusters for $[xPro+H]^+$ (where x = 4, 5, and 6) have a slightly larger drift time by ~0.3% for pure L_{D7}-proline clusters compared to that for pure L-proline clusters. This slight increase in drift time is likely because the isotopically labeled proline clusters are larger in mass than L-proline clusters. Typically, the experimental reproducibility between mobility experiments (recorded as separate data sets) is within 1%, but here it is possible to draw conclusions about proline clusters with drift time differences of less than 1% because these clusters are measured within the same data set. As expected, the same drift time trend is observed for

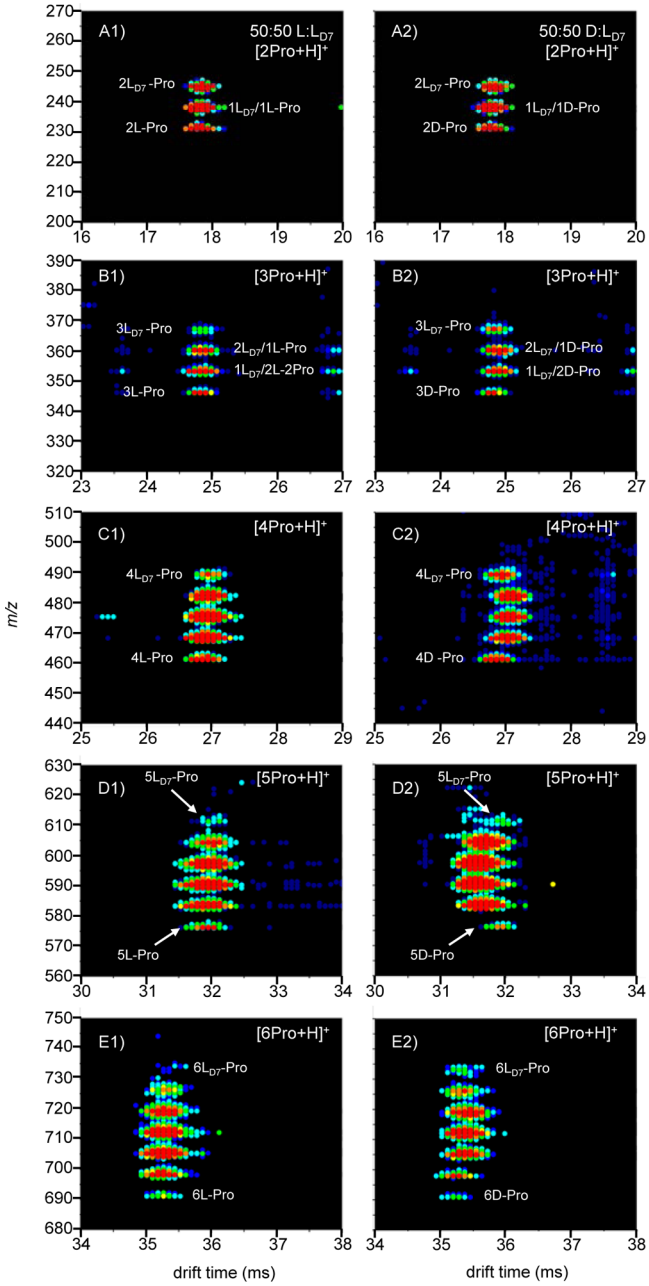

Figure 1. Nested $t_D(m/z)$ plots for electrosprayed solutions containing deuterated L-proline ($HN(CD_2)_3CD$)COOH). Distributions in the first (A1–E1) and second (A2–E2) columns correspond to $[xPro+H]^+$ (where x = 2–6) clusters formed from enantiopure (50:50 L:L_{D7}) and racemic (50:50 L_{D7}:D) solutions, respectively. The arbitrary intensity scheme represents the most intense features in red and the least intense features in navy.

dx.doi.org/10.1021/jp3069915 | J. Phys. Chem. B 2012, 116, 11442–11446

homochiral D (0 L_{D7}) and L_{D7} (x L_{D7}) clusters formed from the racemic solution.

For $[x\text{Pro+H}]^+$ (where x = 2 and 3), enantiopure mixed clusters (composed of both L- and L_{D7}-proline subunits) have the same drift times as pure L and pure L_{D7} clusters. For $[x\text{Pro+H}]^+$ (where x = 4, 5, and 6), drift times of enantiopure clusters composed of isotopically labeled and unlabeled L-proline subunits formed from enantiopure solution slightly increase as the ratio of L_{D7} to L subunits within each cluster increases. These differences are all smaller than ~0.3%, consistent with the effect of incorporating deuterated proline, as described above. The same trend is also observed for the 1L_{D7}:1D-proline cluster produced from electrospraying the racemic solution; this species has the same drift time as the 2L_{D7} and 2D cluster. However, other mixed clusters composed of D- and L_{D7}-proline formed from the racemic solution do not conform to the same trend observed for the clusters formed from the enantiopure solution.

As observed in Figure 1, the 3D-proline cluster has a drift time of 24.82 ms, and both the 1L_{D7}:2D-proline and 2L_{D7}:1D-proline clusters have a drift time of 24.90 ms. The ~0.3% increase in drift time between heterochiral and homochiral $[3\text{Pro+H}]^+$ clusters suggests that the packing of L_{D7}- and D-prolines favors a larger arrangement than the packing of clusters formed from only L- or D-proline. This packing trend is not observed for $[3\text{Pro+H}]^+$ clusters formed from L- and L_{D7}-proline subunits and consequently is not due to the presence of isotopically labeled L_{D7}-proline. The same, but more pronounced, trend is observed for both $[4\text{Pro+H}]^+$ and $[6\text{Pro+H}]^+$ clusters formed from the racemic solution, as described below.

The drift times for 4D-proline and 6D-proline are 26.86 and 35.19 ms, respectively. Those for $[4\text{Pro+H}]^+$ and $[6\text{Pro+H}]^+$ mixed clusters are 27.03 ms for 2L_{D7}:2D-proline and 35.36 ms for 3L_{D7}:3D-proline. These drift time measurements indicate that $[4\text{Pro+H}]^+$ and $[6\text{Pro+H}]^+$ mixed L_{D7}- and D- clusters pack into a larger geometry (by 0.6% and 0.5% respectively) than clusters composed of only D-proline. The opposite trend is observed for $[5\text{Pro+H}]^+$ composed of L_{D7}- and D-proline subunits. Previous isotopically labeled experiments[14,15] suggest that 4L:1D and 1L:4D are the preferred $[5\text{Pro+H}]^+$ clusters formed from the racemic solution. Heterochiral 1L_{D7}:4D_7-proline traverses the drift tube with a drift time of 31.62 ms, while the homochiral 5D-proline cluster has a drift time of 31.87 ms. This ~0.8% difference in drift time suggests that the homochiral $[5\text{Pro+H}]^+$ clusters pack into a larger geometry than clusters composed of mixed L_{D7}- and D-proline (heterochiral clusters).

To analyze the packing of the singly charged proline clusters, it is instructive to consider their chiral preferences. Recently, we reported that small, singly charged clusters of L- and D-proline display an oscillation in chiral preference.[14] We hypothesized that the origin of this trend could be attributed to the existence of L- and D-domains within a cluster with homochiral or heterochiral preference.[14,15] On the basis of these previous findings, we know that $[2\text{Pro+H}]^+$ and $[3\text{Pro+H}]^+$ clusters have a very small heterochiral preference and can be considered achiral. Furthermore, the mixed L_{D7}- and D-proline clusters (heterochiral clusters) of these two singly charged proline clusters have very similar drift profiles compared to the homochiral clusters. One possible explanation for this is that $[2\text{Pro+H}]^+$ and $[3\text{Pro+H}]^+$ clusters pack into similar geometries with just D-proline or with a mixture of L_{D7}- and D-proline subunits and thus have no energetic preference to form homochiral or heterochiral clusters.

A similar argument can be made for $[4\text{Pro+H}]^+$ and $[6\text{Pro+H}]^+$ clusters that have a homochiral preference.[14] Both of these clusters have smaller drift times for homochiral clusters than for heterochiral clusters. Furthermore, previous isotopically labeled experiments[14,15] show that homochiral clusters for $[4\text{Pro+H}]^+$ and $[6\text{Pro+H}]^+$ occur in greater abundance than the mixed L_{D7}- and D-proline clusters. Together, these results suggest that $[4\text{Pro+H}]^+$ and $[6\text{Pro+H}]^+$ clusters preferentially pack into tighter geometries composed of enantiopure proline.

Previous work by Holliday et al.[14] shows that $[5\text{Pro+H}]^+$ has a heterochiral preference, with 4L:1D or 1L:4D clusters being the most favored. Ion mobility analysis reveals that $[5\text{Pro+H}]^+$ ions are more compact for heterochiral clusters than for enantiopure clusters. It is possible that the heterochiral preference for the $[5\text{Pro+H}]^+$ cluster is related to the packing preference of proline residues. In this example, the more compact heterochiral clusters are also the more favored clusters.

Theoretical Collision Cross Sections (ccs). To further explore the idea that the more efficient packing of L- and D-proline residues is associated with the chiral preference of the cluster, we have modeled the homochirally preferring $[4\text{Pro+H}]^+$ cluster and the heterochirally preferring $[5\text{Pro+H}]^+$ cluster. Gas-phase ion structures can be studied by comparing experimental ccs calculated from ion mobility measurements with theoretical ccs derived for structures obtained from molecular modeling.[9,13] To study the packing trends of clusters with homochiral and heterochiral preference, a series of structures was constructed and energy minimized. The modeled structures were converted to ccs using the trajectory method.[34,35] The theoretical ccs shown in Figure 2 (black) represent average ccs for a series of modeled structures that are within ±1.5% of the experimentally determined ccs (red).

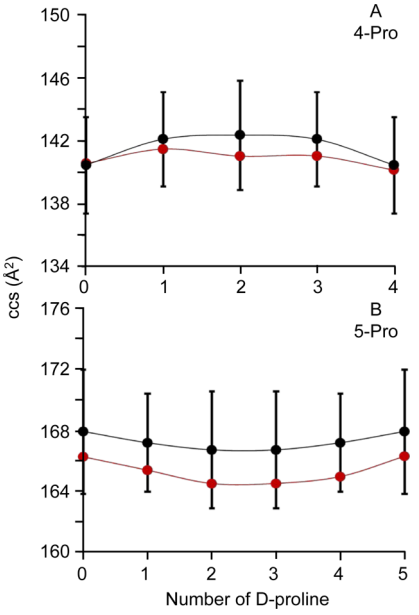

Figure 2. Comparison of theoretical (black) and experimental (red) collision cross sections for $[4\text{Pro+H}]^+$ (A) and $[5\text{Pro+H}]^+$ (B) clusters. Theoretical collision cross sections are calculated using the trajectory method for structures constructed using molecular modeling.

dx.doi.org/10.1021/jp3069915 | J. Phys. Chem. B 2012, 116, 11442–11446

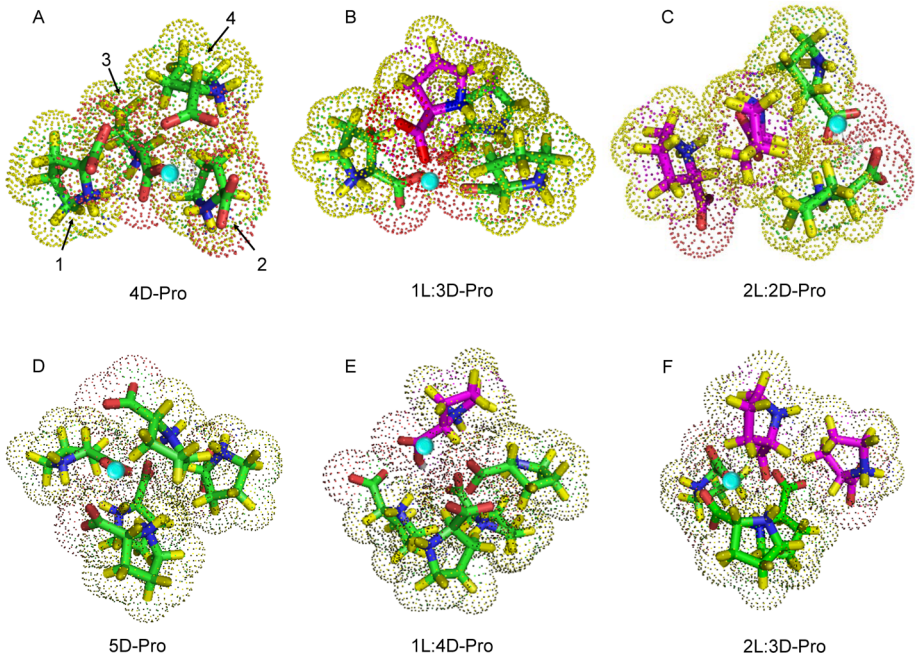

Figure 3. Hypothetical structures for homochiral preferring $[4Pro+H]^+$ clusters composed of 4D-proline (A), 1L:3D-proline (B), and 2L:2D-proline (C), and heterochiral preferring $[5Pro+H]^+$clusters composed of 5D-proline (D), 1L:4D-proline (E), and 2L:3D-proline (F). Note that proline subunits shown in green correspond to D-proline, and subunits shown in magenta correspond to L-proline.

The packing trend determined using molecular modeling for heterochiral and homochiral clusters follows the same trend measured experimentally. Homochiral $[4Pro+H]^+$ clusters pack to form more compact structures than heterochiral clusters. Heterochiral $[5Pro+H]^+$ clusters pack to form more compact structures than homochiral clusters. Error bars for the theoretical cross sections are approximately ±3.0%.

Packing of L- and D-Proline Subunits for $[4Pro+H]^+$ and $[5Pro+H]^+$ Clusters. Figure 3 shows examples of energy minimized structures that suggest how L- and D-proline subunits may pack to form more compact or larger geometries for $[4Pro+H]^+$ and $[5Pro+H]^+$ clusters. The 4D-proline cluster (homochiral) is shown arranged into tetrahedral type geometry. One possible explanation for why this cluster is more compact than the heterochiral $[4Pro+H]^+$ clusters is because it forms more efficient hydrogen bonding between the proline subunits. For example, the 4D-proline cluster shows a stacking of prolines 1, 2, and 3 that favor hydrogen bonding interactions between amine groups present in proline subunits 1 and 2 and the carboxyl group in proline 3. However, the subunits in 1L:3D-proline and 2L:2D-proline clusters are not as efficiently stacked and thus form slightly larger geometries with slightly larger ccs. It is important to note that structures shown in Figure 3 are not absolute but are examples that may help explain how packing can influence the geometry and consequently the ccs of a cluster.

Clusters for $[5Pro+H]^+$ ions assemble into a more compact geometry for racemic clusters than enantiopure clusters. For example, 2L:3D-proline clusters assume a more compact geometry with ccs of 164.5 $Å^2$ than 5D-proline clusters with ccs of 166.3 $Å^2$. Previous results by Clemmer et al.[14,15] show that the 1L:4D-proline cluster is the more prevalent cluster, despite the fact that its ccs (165.0 $Å^2$) is slightly larger than the ccs for the 2L:3D-proline cluster. However, both 1L:4D- and 2L:3D-proline clusters are preferred over 5D-proline clusters. Most likely, the optimal cluster composition is influenced by intermolecular forces that result in more efficient packing of the cluster. It is these interactions that influence the structure and stability of each cluster.

■ CONCLUSION

Collision cross sections of enantiopure and racemic clusters have been examined with IMS-MS and molecular modeling techniques. These results suggest that for small singly charged proline clusters where x = 2−6, the chiral preference of each cluster is related to the packing efficiency of individual proline subunits. For achiral clusters (x = 2 and 3), racemic and enantiopure clusters have very similar packing trends. For clusters with homochiral preference (x = 4 and 6), homochiral clusters have more compact geometries than heterochiral clusters. For $[5Pro+H]^+$ clusters with heterochiral preference, the heterochiral clusters have more compact geometries than homochiral clusters. Molecular modeling of $[4Pro+H]^+$ and $[5Pro+H]^+$ clusters confirms the trends observed experimentally. Together these results suggest that the packing arrangement of each singly charged proline cluster influences its achiral, homochiral, or heterochiral preference.

■ AUTHOR INFORMATION

Corresponding Author

*E-mail: ahollid1@swarthmore.edu (A.E.H.); clemmer@indiana.edu (D.E.C.).

Present Address

[§]Department of Chemistry, West Virginia University, Morgantown, West Virginia 26506, United States.

Notes

The authors declare no competing financial interest.

■ ACKNOWLEDGMENTS

The authors wish to acknowledge funding from the Indiana University MetaCyt initiative funded from the Lilly Endowment.

■ REFERENCES

(1) Nanita, S. C.; Cooks, R. G. *Angew. Chem., Int. Ed.* **2006**, *45*, 554−569.
(2) Pérez-García, L.; Amabilino, D. B. *Chem. Soc. Rev.* **2002**, *31*, 342−356.
(3) Cintas, P. *Angew. Chem., Int. Ed.* **2002**, *41*, 1139−1145.
(4) Cooks, R. G.; Zhang, D.; Koch, J. J.; Gozzo, F. C.; Eberlin, M. N. *Anal. Chem.* **2001**, *73*, 3646−3655.
(5) Hodyss, R.; Julian, R. R.; Beauchamp, J. L. *Chirality* **2001**, *13*, 703−706.
(6) Concina, B.; Hvelplund, P.; Nielsen, A. B.; Nielsen, S. B.; Liu, B.; Tomita, S. *J. Am. Soc. Mass Spectrom.* **2006**, *17*, 275−279.
(7) Nemes, P.; Schlosser, G.; Vékey, K. J. *J. Mass Spectrom.* **2005**, *40*, 43−49.
(8) Counterman, A. E.; Clemmer, D. E. *J. Phys. Chem. B* **2001**, *105*, 8092−8096.
(9) Julian, R. R.; Hodyss, R.; Kinnear, B.; Jarrold, M. F.; Beauchamp, J. L. *J. Phys. Chem. B* **2002**, *106*, 1219−1228.
(10) Julian, R. R.; Myung, S.; Clemmer, D. E. *J. Am. Chem. Soc.* **2004**, *126*, 4110−4111.
(11) Myung, S.; Fioroni, M.; Julian, R. R.; Koeniger, S. L.; Baik, M.-H.; Clemmer, D. E. *J. Am. Chem. Soc.* **2006**, *128*, 10833−10839.
(12) Myung, S.; Julian, R. R.; Nanita, S. C.; Cooks, R. G.; Clemmer, D. E. *J. Phys. Chem. B* **2004**, *108*, 6105−6111.
(13) Myung, S.; Lorton, K. P.; Merenbloom, S. I.; Fioroni, M.; Koeniger, S. L.; Julian, R. R.; Baik, M. H.; Clemmer, D. E. *J. Am. Chem. Soc.* **2006**, *128*, 15988−15989.
(14) Holliday, A. E; Atlasevich, N.; Myung, S.; Plasencia, M. D.; Valentine, S. J.; Clemmer, D. E. *J. Phys. Chem. A.* **2012**, DOI: http://dx.doi.org/10.1021/jp302677n.
(15) Atlasevich, N.; Holliday, A.; Valentine, S. J.; Clemmer, D. E. *J. Phys. Chem. B* **2012**, *116*, 7644−7651.
(16) Julian, R. R.; Myung, S.; Clemmer, D. E. *J. Phys. Chem. B* **2005**, *109*, 440−444.
(17) Koch, K. J.; Gozzo, F. C.; Zhang, D.; Eberlin, M. N.; Cooks, R. G. *Chem. Commun.* **2001**, 1854−1855.
(18) Schalley, C. A.; Weis, P. *Int. J. Mass Spectrom.* **2002**, *221*, 9−19.
(19) Costa, A. B.; Cooks, R. G. *Phys. Chem. Chem. Phys.* **2011**, *13*, 877−885.
(20) Mason, E. A.; McDaniel, E. W. *Transport Properties of Ions in Gases*; Wiley: New York, 1988.
(21) St. Louis, R. H.; Hill, H. H. *Crit. Rev. Anal. Chem.* **1990**, *21*, 321−355.
(22) Hoaglund Hyzer, C. S.; Counterman, A. E.; Clemmer, D. E. *Chem. Rev.* **1999**, *99*, 3037−3079.
(23) Wittmer, D.; Luckenbill, B. K.; Hill, H. H.; Chen, Y. H. *Anal. Chem.* **1994**, *66*, 2348−2355.
(24) von Helden, G.; Wyttenbach, T.; Bowers, M. T. *Science* **1995**, *267*, 1483−1485.
(25) Chen, Y. H.; Siems, W. F.; Hill, H. H. *J. Anal. Chim. Acta* **1996**, *334*, 75−84.
(26) Hoaglund, C. S.; Valentine, S. J.; Sporleder, C. R.; Reilly, J. P.; Clemmer, D. E. *Anal. Chem.* **1998**, *70*, 2236−2242.
(27) Hoaglund-Hyzer, C. S.; Li, J.; Clemmer, D. E. *Anal. Chem.* **2000**, *72*, 2737−2740.
(28) Bluhm, B. K.; Gillig, K. J.; Russell, D. H. *Rev. Sci. Instrum.* **2000**, *71*, 4078−4086.
(29) Tang, K.; Shvartsburg, A. A.; Lee, H. N.; Prior, D. C.; Buschbach, M. A.; Li, F. M.; Tolmachev, A. V.; Anderson, G. A.; Smith, R. D. *Anal. Chem.* **2005**, *77*, 3330−3339.
(30) Revercomb, H. E.; Mason, E. A. *Anal. Chem.* **1975**, *47*, 970−983.
(31) Wyttenbach, T.; von Helden, G.; Batka, J. J.; Carlat, D.; Bowers, M. T. *J. Am. Soc. Mass Spectrom.* **1997**, *8*, 275−282.
(32) Merenbloom, S. I.; Koeniger, S. L.; Valentine, S. J.; Plasencia, M. D.; Clemmer, D. E. *Anal. Chem.* **2006**, *78*, 2802−2809.
(33) Koeniger, S. L.; Merenbloom, S. I.; Valentine, S. J.; Jarrold, M. F.; Udseth, H.; Smith, R. D.; Clemmer, D. E. *Anal. Chem.* **2006**, *78*, 4161−4174.
(34) Shvartsburg, A. A.; Jarrold, M. F. *Chem. Phys. Lett.* **1996**, *261*, 86−91.
(35) Mesleh, M. F.; Hunter, J. M.; Shvartsburg, A. A.; Schatz, G. C.; Jarrold, M. F. *J. Phys. Chem.* **1996**, *100*, 16082−16086.